EFFECT OF THERMALIZED ELECTRONS ON THE ENERGY RELEASE OF A HIGH-CURRENT ELECTRON BEAM IN A TARGET

G. E. Gorelik, A. I. Pobitko, S. G. Rozin, and L. I. Sal'nikov

UDC 537.533.7

The Monte Carlo method is used to study the effect of the self-magnetic field of thermalized electrons on the energy release in metal targets.

The effect of the self-magnetic field of a high-current electron beam (HEB) on the passage of the beam through matter was the subject of a number of recent studies [1-4]. Some of them consider only the magnetic field of fast electrons (for metals) [3, 4] and others (for dielectrics) consider only the effect of thermalized electrons on the self-electric field [5]. Yalovets [2] demonstrated that the current of thermalized electrons must also be taken into account in metals, where because of the high conductivity it is rather large, despite the weakness of the electric field.

Here we study the effect of the current of thermalized electrons on the energy-loss distribution of fast electrons of a HBE in metal targets. The problem is solved in the quasi-steady approximation, i.e., we assume that the relaxation time of fast electrons is substantially shorter than the characteristic time of beam-parameter variation. Moreover, we assume that the transient terms in the Maxwell equations can be disregarded.

When these assumptions are made and the space-charge field of the beam is ignored the problem reduces to the common solution of the transport equation for relativistic beams in the material and the corresponding Maxwell's equations [1, 2].

The self-magnetic field of the HEB in the material is described by

$$[\nabla \mathbf{B}] = \mu_0 \mu (\mathbf{j}_b + \mathbf{j}_t), \tag{1}$$

where μ is henceforth assumed to be close to unity since the material becomes diamagnetic under the effect of the HEB [2]. Using Ohm's law $\mathbf{j}_t = -\sigma \nabla \varphi_t$, the continuity equation $\nabla (\mathbf{j}_b + \mathbf{j}_t) = 0$ and the known relation for the rate of fast-electron thermalization N($\nabla \mathbf{j}_b = -eN$) we easily obtain an equation for the electric-field potential φ_t of the thermalized electrons:

$$\Delta \varphi_t = -\frac{eN}{\sigma}. \tag{2}$$

The potential was assumed to be zero at the surface of the target,

$$\varphi_t(\rho, z) = 0, \ (\rho, z) \in \Gamma_\Omega, \tag{3}$$

and N and j_b were found by solving the transport equation [3, 4]. The path of the beam electrons was calculated by the Monte Carlo method using the scheme of continuous energy loss and scattering on a segment from the Goudsmitt–Sanderson formulas [6]. If the electron energy dropped below some minimum value, which was chosen so that the residual electron range would be less than half the spacing of the net, the electron was no longer tracked and was assumed to have been thermalized. The number of paths of fast electrons tracked was of the order of a thousand.

The effect of the self-magnetic field was taken into account by an additional change in the particle momentum at the end of the range in accordance with the Lorentz equation,

---

L. V. Lykov Institute of Heat and Mass Transfer, Academy of Sciences of the Belorussian SSR. Institute of Nuclear Power, Academy of Sciences of the Belorussian SSR, Minsk. Translated from Inzhenerno-fizicheskii Zhurnal, Vol. 61, No. 3, pp. 443-446, September, 1991. Original article submitted September 13, 1990.

 0022-0841/91/6103-1130$12.50

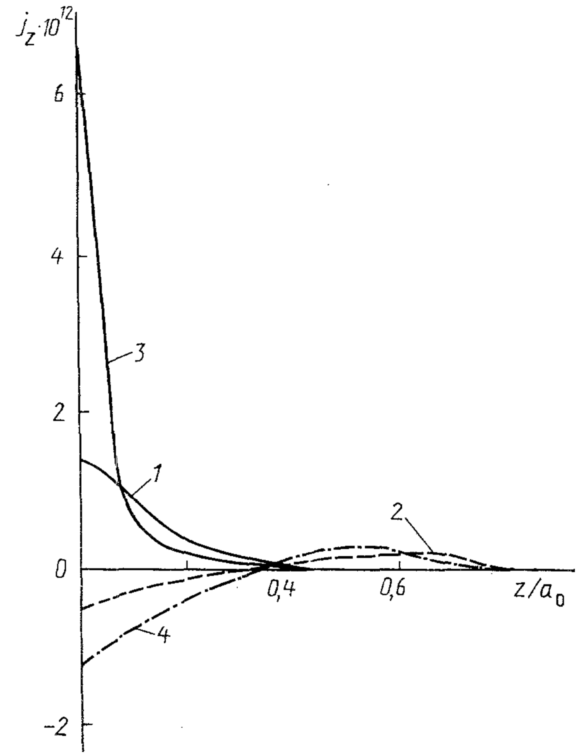

Fig. 1. Current-density distribution along the thickness of the target (E_0 = 1 MeV, N_0 = 1000, $r_0 = 2.1 \cdot 10^{-3}$ m, $H = 4.2 \cdot 10^{-3}$ m, $\sigma = (\Omega \cdot m)^{-1}$: 1, 3) current density of fast electrons at $I = 5 \cdot 10^4$ A and $I = 10^5$ A, respectively; 2, 4) current density of thermalized electrons at $I = 5 \cdot 10^4$ A and $I = 10^5$ A, respectively. j_z, A/m³.

$$m \frac{d}{dt}(\beta\gamma) = -e[\beta \mathbf{B}]. \tag{4}$$

The problem was solved in the cylindrical coordinate system for the case of axisymmetry. As in [3, 4], we included only the aximuthal component B_φ, of the magnetic field, which was determined by the longitudinal component of the current-density vector j_z. The density j_z was determined as the sum of the longitudinal components of the current-density vectors of fast and thermalized electrons. The values of j_{bz} were calculated by the flux tube method [7] and j_{tz}, by solving the system (2)-(3) and Ohm's law. The Poisson equation (2) with boundary condition (3) was solved with difference schemes, using the Pismen–Reckford method of variable directions [8]. The essence of the method is that intermediate values are calculated along with the main values of the desired functions.

The calculations were performed on a BÉSM-6 computer for a high-current electron beam of radius $r_0 = (1\text{-}2) \cdot 10^{-3}$ m, with a current $I = 10^3\text{-}10^6$ A, and electron energy E_0 = 1 MeV at normal incidence of the beam on an aluminum target with thickness $H = 4.2 \cdot 10^{-3}$ m and conductivity $\sigma = 10^3\text{-}10^5$ $(\Omega \cdot m)^{-1}$.

Figure 1 shows the calculated values of the current density of both thermalized and fast electrons in the paraxial region. The depth in fractions of electron range is laid off along the abscissa axis and the z component of the current-density vector in A/Am³ is laid off along the ordinate axis. The calculations showed that within the framework of the assumptions made, the current density of the thermalized electrons depends weakly on the conductivity of the material. We see from Fig. 1 that at small depths ($z \leq 0.3\ a_0$) the thermalized-electron current is counter to the beam current, thus slightly decreasing the self-magnetic field in this region. At larger depths ($z > 0.3\ a_0$) the magnetic field forms mainly because of the thermalized-electron current, directed along the beam. With increasing beam current the relative fraction of the thermalized-electron current density decreases at the surface.

Figure 2 shows the calculated values of the energy loss as a function of the HEB current. The distributions along the thickness of the target are shown. The relative density

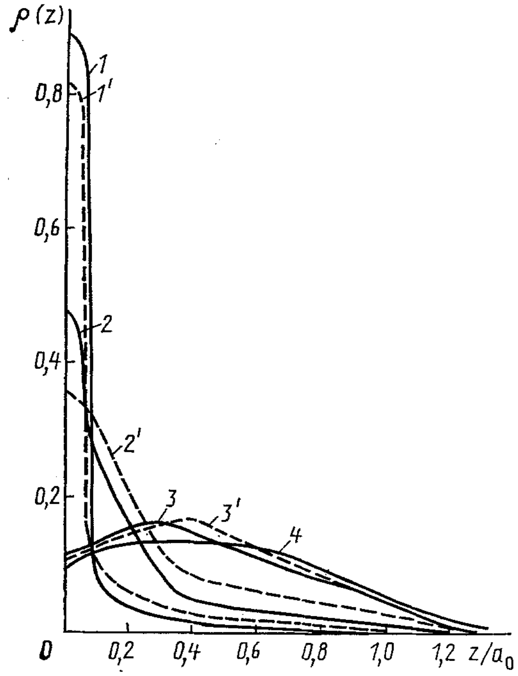

Fig. 2. Distribution of beam energy loss along the thickness of an aluminum sample ($E_0 = 1$ MeV, beam radius $r_0 = 2 \cdot 10^{-3}$ m): 1, 2, 3, 4 correspond to currents $I = 10^5$ A, $5 \cdot 10^4$ A, 10^4 A, and 10^3 A without allowance for the thermalized electrons; 1', 2', 3' correspond to currents $I = 10^5$ A, $5 \cdot 10^4$ A, and 10^4 A with allowance for the thermalized electrons.

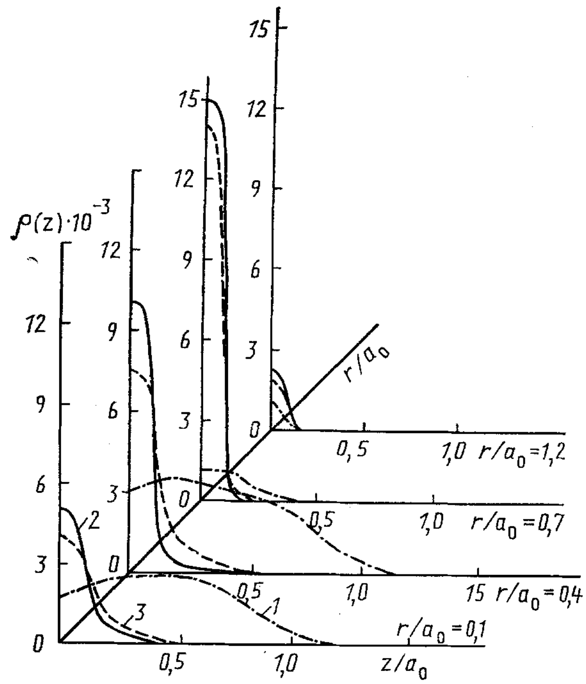

Fig. 3. Profiles of the spatial distribution of energy loss in an aluminum target for a cylindrical beam of radius $r_0 = 10^{-3}$ m ($E_0 = 1$ MeV): 1) at $I = 10^3$ A; 2) $I = 10^5$ A without allowance for thermalized electrons; 3) $I = 10^5$ A with allowance for thermalized electrons.

of energy release $\rho(z) = (r_0/P_0)(dP/dz)$ ($P = IE$) is laid off along the ordinate axis and the depth, in units of electron range, is laid off along the abscissa axis. Figure 2 shows that the effect of the thermalized-electron current is substantial in a certain range of values of the HEB current. At low currents $I < 10^4$ A the thermalized-electron current has virtually no effect on the energy release because the self-magnetic field is insignificant (curve 4). With increasing beam current the contribution of the thermalized electrons to the formation of the self-magnetic field grows and so does their effect on the nature of the energy release (curves 2, 2' and 3, 3'). With a further increase in the beam current the region of vigorous energy release contracts toward the surface, i.e., into the region where the relative fraction of the thermalized-electron current decreases (see Fig. 1). Because of this the effect of the thermalized-electron current on the formation of the region of energy release becomes weaker (curves 1, 1').

From Fig. 3, which shows the energy release in cylindrical layers of the target, we see that the effect of the thermalized-electron current on the energy-loss distribution is most pronounced in the middle layers with $r \sim 0.4\text{-}0.6\ a_0$.

NOTATION

a_0, electron range, $a_0 = 2.04$ cm, at $E_0 = 1$ MeV; β, relative electron velocity; $\gamma = (1 - \beta^2)^{-1/2}$; e, electron charge; m, electron mass; B, magnetic induciton; B_φ, azimuthal component of the magnetic induction; N, thermalization rate of fast electrons; N_0, number of cases; E_0, initial electron energy; $P = IE$, E is the acceleration voltage (MV), numerically equal to the electron energy (MeV); I, beam current; r_0, beam radius; $\rho(z)$, relative density of energy release; $\rho(z) = (r_0/P_0)(dP/dz)$; H, target thickness; σ, target conductivity; μ_0, magnetic constant; μ, relative magnetic permeability of the medium; Ω, boundary of computation region; φ_t, potential of electric field of thermalized electrons; j_t and j_{bz}, current-density vector of the fast beam electrons and its longitudinal component; j_t and j_{tz}, vector of thermalized-electron current density and its longitudinal component; and j_z, longitudinal component of the beam density vector.

LITERATURE CITED

1. V. I. Boiko and V. V. Evstigneev, Introduction to the Physics of the Interaction of High-Current Beams of Charged Particles with Matter [in Russian], Moscow (1988).
2. A. P. Yalovets, Izv. Vyssh. Uchebn. Zaved. SSSR, Fiz., No. 4, 124 (1986); No. 7409-V85, Deposited at All-Union Institute of Scientific and Technical Information, October 23 (1985).
3. V. I. Boiko, E. A. Gorbachev, and V. V. Evstigneev, Fiz. Plazmy, 9, No. 4, 764-769 (1983).
4. G. E. Gorelik, S. I. Legovich, and S. G. Rozin, Inzh.-fiz. Zh., 57, No. 6, 977-980 (1987).
5. V. I. Boiko, E. A. Gorbachev, and V. V. Evstigneev, Izv. Vyssh. Uchebn. Zaved. SSSR, Fiz., No. 5, 122-124 (1981).
6. G. E. Gorelik and S. G. Rozin, Inzh.-fiz. Zh., 22, No. 6, 1110-1113 (1972).
7. A. S. Roshal', Simulation of Charged Beams [in Russian], Moscow (1979).
8. A. A. Samarskii and E. S. Nikolaev, Methods of Solving Net-Point Equations [in Russian], Moscow (1978).